XII International Conference on Computational Plasticity. Fundamentals and Applications
COMPLAS XII
E. Oñate, D.R.J. Owen, D. Peric and B. Suárez(Eds)

MODELING OF DUCTILE DAMAGE USING NUMERICAL ANALYSES ON THE MICRO-SCALE

MICHAEL BRÜNIG, STEFFEN GERKE AND VANESSA HAGENBROCK

Institute for Mechanics and Structural Analysis
Universität der Bundeswehr München
Werner-Heisenberg-Weg 39, D-85577 Neubiberg, Germany
e-mail: michael.bruenig@unibw.de, www.unibw.de/baumechanik

Key words: Ductile Materials, Damage and Fracture, Stress State Dependence, Micro-mechanical Numerical Simulations.

Summary. *The presentation deals with a continuum damage model which has been generalized to take into account the effect of stress state on damage criteria as well as on evolution equations of damage strains. It is based on the introduction of damaged and corresponding undamaged configurations. Plastic behavior is modeled by a yield criterion and a flow rule formulated in the effective stress space (undamaged configurations). In a similar way, damage behavior is governed by a damage criterion and a damage rule considering the damaged configurations. Different branches of the damage criterion are considered corresponding to various damage mechanisms depending on stress intensity, stress triaxiality and the Lode parameter. Experiments with carefully designed specimens are performed and the test results are used to identify basic material parameters. However, it is not possible to determine all parameters based on these tension and shear tests. To be able to get more insight in the complex damage behavior under different loading conditions, additional series of micro-mechanical numerical analyses of void containing unit cells have been performed. These finite element calculations on the micro-level cover a wide range of stress triaxialities and Lode parameters in the tension, shear and compression domain. The numerical results are used to show general trends, to develop equations for the stress-state-dependent damage criteria, to propose evolution equations of damage strains, and to identify parameters of the continuum model.*

1 INTRODUCTION

Efficient and accurate material models proposing inelastic behavior, damage and fracture of ductile metals are evident in structural and computational mechanics and corresponding numerical simulations. In this context, a large number of widely used elastic-plastic constitutive approaches as well as associated robust and efficient algorithms have been presented in many conferences and discussed in the literature. However, in many ductile materials damage and fracture have been observed with increasing inelastic deformations leading to final failure of engineering structures. Therefore, various continuum models have been proposed to take into account these deteriorating effects. These approaches model in a

phenomenological way growth and coalescence of micro-defects as well as corresponding macroscopic material softening during damage and fracture processes under general loading conditions. They are based on internal scalar or tensorial damage variables whose increase is governed by evolution laws. Critical values of these damage variables may be seen as major parameters characterizing the onset of failure.

It has been recently discussed in the literature that the stress state remarkably affects the damage and failure mechanisms. Thus, besides the stress intensity, the stress triaxiality and the Lode parameter are important factors controlling initiation and evolution of ductile damage and fracture. These effects can be examined by experiments and corresponding numerical simulations of a series of tests with carefully designed and differently loaded specimens taking into account a wide range of stress states [1-8].

However, it is not possible to detect in detail damage and failure mechanisms on the micro-scale affecting the macroscopic behavior of materials by currently available experimental techniques. Therefore, micro-mechanical approaches have been used to solve boundary-value problems of representative volume elements with micro-structural details helping to develop constitutive equations at the macroscopic level [9-18]. The numerical results have shown that void growth, macroscopic deformation behavior of the representative volume elements and the critical failure strain remarkably depend on the values of the stress triaxiality. On the other hand, the rate of expansion of micro-defects in different directions is sensitive to the Lode parameter. Hence, anisotropy of damage evolution is affected by the stress state.

In many publications, authors only examine void growth and coalescence in regions with high hydrostatic stress appearing, for example, ahead of a crack tip. These results are only valid for moderate or high stress triaxialities where the effect of the Lode parameteron ductile damage and failure behavior is marginal. Therefore, in the present paper further numerical calculations will be discussed. Numerical unit cell simulations on the micro-scale covering a wide range of loading conditions in the tension, shear and compression regimes deliver detailed information on damage and failure mechanisms in ductile metals for a wide range of stress states. The numerical results are used to develop and to validate stress-state-dependent damage and failure criteria taking into account different branches corresponding to various damage and failure modes depending on both the stress triaxiality and the Lode parameter.

2 CONTINUUM MODEL

A phenomenological framework based on a continuum model is used to describe the inelastic deformation behavior of ductile solids including anisotropic damage caused by individual micro-defects and their interactions [19]. The approach is based on the introduction of damaged as well as fictitious undamaged configurations. The kinematics lead to the additive decomposition of the strain rate tensor into elastic, plastic and damage parts. Furthermore, the fictitious undamaged configurations are considered to formulate the constitutive equations modeling the effective elastic-plastic deformation behavior of the undamaged matrix material. Elastic behavior is characterized by an isotropic hyperelastic law taking into account constant shear and bulk modulus. It has been observed in experiments that plastic behavior is also affected by the stress state and, thus, the stress-triaxiality dependent plastic yielding of the undamaged matrix material is assumed to be governed by the Drucker-Prager-type yield condition

$$f^{\mathrm{pl}} = \sqrt{\bar{J}_2} - c\left(1 - \frac{a}{c}\bar{I}_1\right) = 0 \tag{1}$$

where $\bar{I}_1$ and $\bar{J}_2$ are the first and the second deviatoric invariants of the effective stress tensor (referred to the undamaged configurations), c denotes the strength coefficient and a represents the hydrostatic stress coefficient of the matrix material where a/c is a constant material parameter. Since plastic volumetric strains have been shown to be marginal a non-associated flow rule is used. Therefore, the effective plastic strain rate

$$\dot{\mathbf{H}}^{\mathrm{pl}} = \dot{\gamma}\frac{1}{\sqrt{2\bar{J}_2}}\mathrm{dev}\bar{\mathbf{T}} \tag{2}$$

describes the isochoric evolution of plastic strains. In Eq. (2), $\dot{\gamma}$ is a non-negative scalar-valued factor denoting the equivalent plastic strain rate taken into account in the present material model.

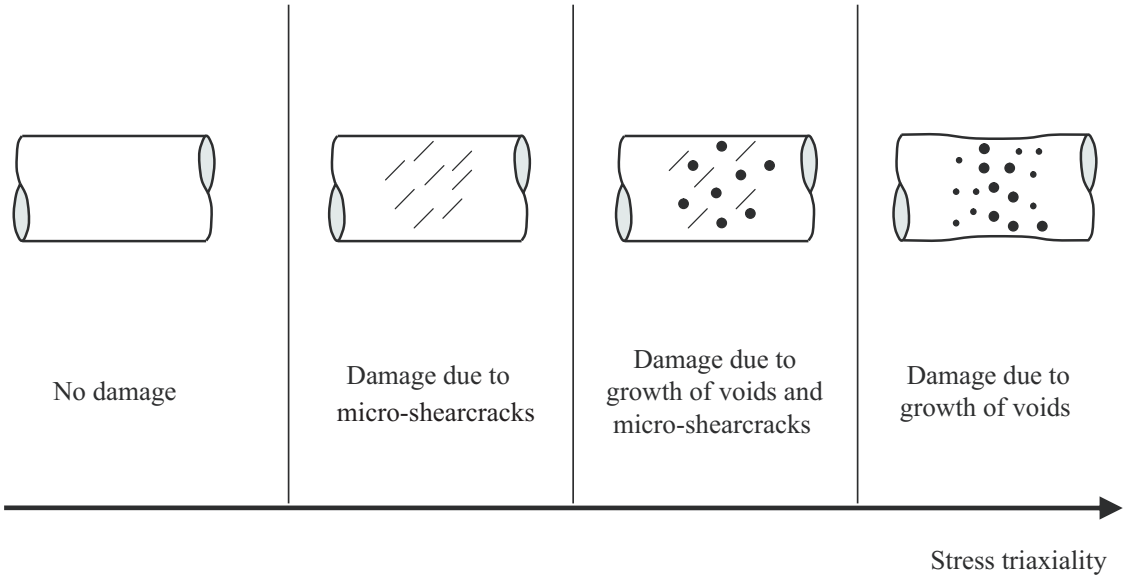

Figure 1: Damage mechanisms

Moreover, formulation of elastic and damage constitutive equations characterizing the deformation behavior of the damaged aggregate is performed with respect to the corresponding anisotropically damaged configurations [19]. In particular, to be able to simulate deterioration of elastic properties due to formation and growth of micro-defects, a generalized elastic-damage law formulated in terms of elastic and damage strain tensors has been proposed. In addition, a damage criterion is considered to characterize onset and continuation of damage during further loading of the material sample. In this context, different damage and failure mechanisms acting on the micro-level leading to final fracture have to be taken into account [2, 18]. This leads to consideration of a wide range of stress triaxialities with different branches (see Fig. 1): damage and failure are caused by growth of voids for large positive stress triaxialities, by formation of micro-shear-cracks in the negative

stress triaxiality regime and by combination of both microscopic mechanisms for low positive stress triaxialities. In addition, for stress states with remarkable hydrostatic pressure, a cut-off value has been proposed below which damage and fracture do not occur [20, 21]. This stress triaxiality dependent concept is taken into account in the present investigation and will be generalized by additional consideration of the Lode parameter.

Therefore, the onset of damage is assumed to be governed by the damage criterion

$$f^{\mathrm{da}} = \alpha I_1 + \beta\sqrt{J_2} - \sigma = 0 \tag{3}$$

where α and β are the stress-state-dependent damage mode parameters, I_1 and J_2 are the first and deviatoric second invariants of the stress tensor (referred to the damaged configurations) and σ represents the damage threshold. In addition, the damage evolution law describes the increase in macroscopic damage strains caused by the simultaneous growth of voids, their coalescence as well as the formation of micro-cracks and micro-shear-cracks:

$$\dot{\mathbf{H}}^{\mathrm{da}} = \dot{\mu}\left(\bar{\alpha}\frac{1}{\sqrt{3}}\mathbf{1} + \bar{\beta}\mathbf{N} + \bar{\delta}\mathbf{M} \right) \tag{4}$$

In Eq. (4), $\bar{\alpha}$, $\bar{\beta}$ and $\bar{\delta}$ are stress-state-dependent kinematic variables describing the portion of volumetric and isochoric damage-based deformations, $\dot{\mu}$ means the equivalent damage strain rate measure, whereas **N** and **M** are the normalized stress tensors:

$$\mathbf{N} = \frac{1}{\sqrt{2J_2}}\mathrm{dev}\tilde{\mathbf{T}} \tag{5}$$

and

$$\mathbf{M} = \frac{1}{\left\|\mathrm{dev}\tilde{\mathbf{S}}\right\|}\mathrm{dev}\tilde{\mathbf{S}} \tag{6}$$

with

$$\mathrm{dev}\tilde{\mathbf{S}} = \mathrm{dev}\tilde{\mathbf{T}}\mathrm{dev}\tilde{\mathbf{T}} - \frac{2}{3}J_2\mathbf{1} \quad . \tag{7}$$

The tensor of rate of damage strains (4) takes into account volumetric and deviatoric parts corresponding to isotropic growth of voids and anisotropic evolution of micro-cracks, respectively.

3 IDENTIFICATION OF MATERIAL PARAMETERS

To be able to identify basic material parameters experiments and corresponding numerical simulations have to be performed. For example, tension and shear tests with smooth and pre-notched specimens taken from aluminum alloys have been discussed by [6]. These experiments cover a wide range of stress triaxialities and, thus, can be used to identify material parameters in stress-state-dependent plasticity and damage models.

In particular, elastic-plastic material parameters are identified using experimental results from tension tests with unnotched specimens. For the aluminum alloy under investigation fitting of experimentally obtained equivalent stress-equivalent strain curves and numerical functions leads to Young's modulus E = 72,000 MPa and Poisson's ratio is taken to be ν = 0.3. Furthermore, work-hardening plastic behavior is modeled by the power-law function for the equivalent stress measure in Eq. (1)

$$c = c_0 \left(\frac{H\gamma}{nc_0} + 1 \right)^n . \tag{8}$$

Fitting the experimental equivalent stress-equivalent plastic strain curves from the uniaxial tension tests of the unnotched specimens leads to the initial yield strength c = 250MPa, the hardening modulus H = 3125 MPa and the hardening exponent n = 0.135. In addition, stress-state-dependent constitutive parameters are identified by examination of test results from experiments with differently notched specimens. In the plastic regime, the hydrostatic stress coefficient in the yield criterion is chosen to be a/c = 0.00005 MPa^{-1}.

Furthermore, onset of damage is identified by an experimental-numerical technique [8]. Load-engineering strain curves obtained from various tests with smooth and differently notched specimens are compared with corresponding elastic-plastic numerical analyses. Beginning of deviation of these curves corresponds to the onset of damage. For the considered aluminum alloy the initial damage threshold is σ = 325 MPa.

The experiments discussed above have been performed with flat specimens taken from thin aluminum sheets. Therefore, only plane stresses are active and, as a consequence, it was not possible to detect the effect of the Lode parameter on the constitutive behavior by experimental techniques. In addition, it is not possible to uniquely identify all material parameters appearing in the equations modeling the damage and failure behavior of ductile metals. To overcome this problem, additional numerical calculations on the micro-level have been performed [17, 18] to be able to study in detail the stress state dependence of the damage and failure mechanisms.

4 NUMERICAL STUDIES ON THE MICRO-SCALE

Numerical simulations on the micro-scale considering parts of materials containing micro-defects will be discussed in this section. The investigation of this prototype problem is motivated by the fact that nucleation, growth and coalescence of micro-defects are the relevant mechanisms leading to damage and failure in solids as well as to deterioration of material properties. In particular, the behavior of representative 2D plane strain elements with cylindrical voids is studied. Symmetry boundary conditions are taken into account simulating periodic distribution of micro-defects under various loading conditions. The numerical results are used to propose damage evolution equations and to identify material parameters in constitutive equations which are motivated by consideration of damage and failure mechanisms on the micro-scale.

Following the ideas discussed in [17, 18] the numerical calculations have been performed using the commercial finite element program ANSYS. Figure 2 shows one fourth of the symmetric cell model with initial porosity of 3% as well as the finite element mesh based on 2662 2D-elements of type Plane 182. Different loading conditions with prescribed macro-scopic normal displacements acting on the outer bounds of the unit cell are taken into account. This allows consideration of different Lode parameters and a wide range of stress triaxialities to be able to study in detail the stress state dependence of various damage and failure mechanisms. In the analyses growth of voids as well as their coalescence is numerically simulated. Based on experimental observations and numerical simulations on the macro-scale [8] the process of coalescence is assumed to start when the damage condition (3) with σ = 340

MPa is fulfilled in one finite element and is numerically modeled by an element erosion technique. In each calculation the balance of mass is controlled and the error here was less than 5%.

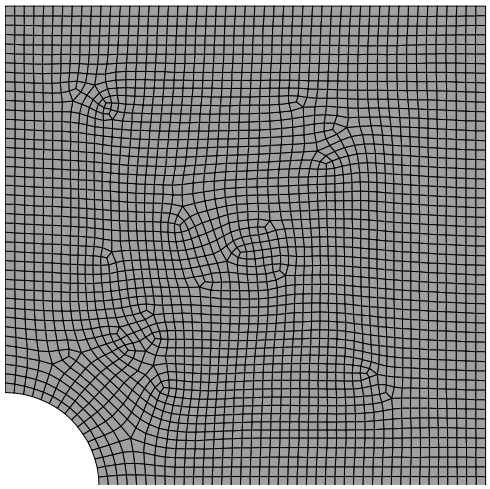

Figure 2: Finite element mesh of one fourth of the unit cell model

In the proposed continuum damage model the damage process is characterized by the evolution of damage strains on the macro-scale caused by changes in size and shape of micro-defects. Based on the kinematic relations discussed in [18] the components in principal directions (i) of the macroscopic strain rate tensor are additively decomposed

$$\dot{H}_{(i)} = \dot{H}^{el}_{(i)} + \dot{H}^{pl}_{(i)} + \dot{H}^{da}_{(i)} \tag{9}$$

into elastic, plastic and damage parts. In the undamaged matrix material of the unit cell only elastic and plastic strain rates occur during loading leading to corresponding macroscopic strain rates

$$\dot{\mathbf{H}}^{ep} = \dot{\mathbf{H}}^{el} + \dot{\mathbf{H}}^{pl} = \frac{1}{V}\int\limits_{V_{matrix}} \left(\dot{\mathbf{h}}^{el} + \dot{\mathbf{h}}^{pl}\right) dv \tag{10}$$

where$V$ represents the current volume of the unit cell and V_{matrix} means the current volume of the matrix material. Since only loading conditions with prescribed macroscopic normal displacements acting on the boundaries are taken into account, only principal values of the respective macroscopic strain rate tensors exist. Thus, with Eq. (9) the principal components of the strain rate tensor (4) can be computed by

$$\dot{H}^{da}_{(i)} = \dot{H}_{(i)} - \dot{H}^{ep}_{(i)} \tag{11}$$

leading to the principal values of the damage strain tensor

$$A^{da}_{(i)} = \int \dot{H}^{da}_{(i)} dt \ . \tag{12}$$

Moreover, the scalar-valued equivalent strain rate measure

$$\dot{\varepsilon}_{eq} = \sqrt{\frac{2}{3}\dot{\mathbf{H}}\cdot\dot{\mathbf{H}}} \tag{13}$$

is introduced to characterize the amount of state of strain rates of the unit cell model on the macro-level leading to the total equivalent strain

$$\varepsilon_{eq} = \int \dot{\varepsilon}_{eq} dt \quad . \tag{14}$$

Figure 3 shows the formation of principal damage strain components during tensile loading in horizontal direction 1 of the void-containing representative volume element (Fig. 2) as well as the damaged unit cell at the final loading stage shortly before the macroscopic crack occurs. In particular, the damage strain in horizontal (loading) direction 1 slightly increases caused by growth of the void. Then, at ε_{eq} = 0.0044 onset of coalescence is numerically predicted. The coalescence process leads to a remarkable increase in damage strain in loading direction. In addition, the damage strain component perpendicular to the loading direction (vertical direction 2) remains very small during the growth of the void and slightly increases during coalescence of voids.The remarkable increase of damage caused by coalescence of the voids is visualized in Fig. 3 showing the remaining finite elements. Horizontal loading of the unit cell leads to formation of a macro-crack normal to the loading direction agreeing well with experimental observations.

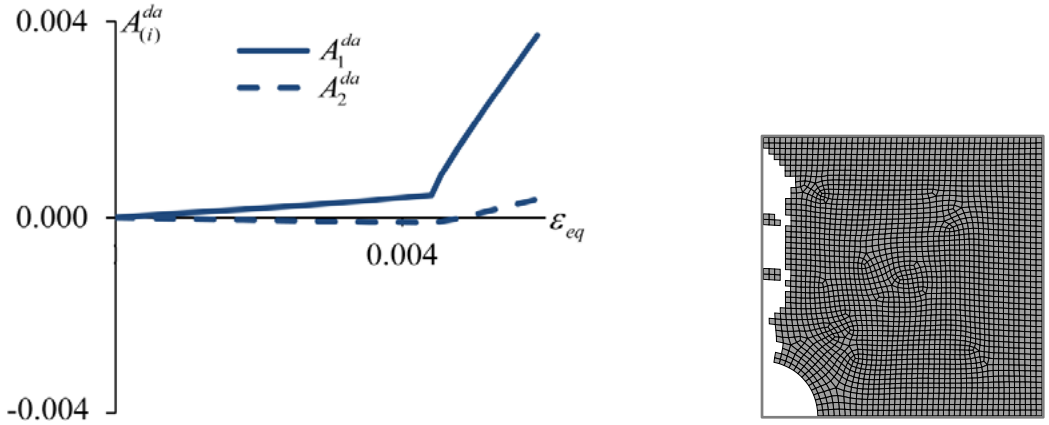

Figure 3: Principal damage strain components vs. equivalent strain in uniaxial tension tests and damaged unit cell

Figure 4 shows formation of principal damage strain components during a shear test as well as the damaged unit cell at the final loading stage shortly before the macroscopic crack occurs. Shear stress state is simulated by tensile loading in horizontal direction 1 and simultaneous compression loading in vertical direction 2. In the first loading stage the damage strains show slight increase in direction 1 and a decrease in direction 2 with the same amount indicating the isochoric change in shape of the initially cylindrical void. Then, at ε_{eq} = 0.0047 onset of coalescence is numerically predicted. The coalescence process leads to a remarkable increase in amount of both principal damage strain components. In addition, the remarkable increase of damage caused by coalescence of the voids is also visualized in Fig. 4 showing the remaining finite elements. Shear loading of the unit cell leads to formation of macro-cracks nearly simultaneously in horizontal and vertical directions.

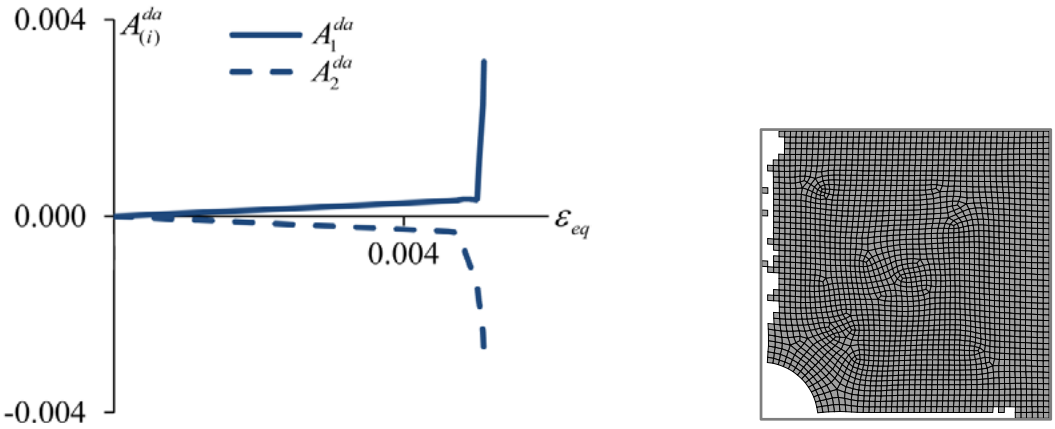

Figure 4: Principal damage strain components vs. equivalent strain in shear tests and damaged unit cell

5 CONCLUSIONS

The effect of stress state on damage and failure behavior has been discussed and has been quantified for the evolution of irreversible strains caused by growth and coalescence of micro-defects. Since the influence of the stress intensity, the stress triaxiality and the Lode parameter on damage and failure behavior cannot be validated by experiments and corresponding macroscopic numerical calculations alone, numerical simulations on the micro-level have been performed to get further information about stress state dependence. In particular, experimental results from tension and shear tests in combination with numerical results obtained from corresponding numerical simulations on the macro-level have been used to identify basic elastic-plastic material parameters as well as the onset of damage. Details of functions modeling the stress state dependent damage behavior are based on unit cell model calculations considering a wide range of stress triaxialities and Lode parameters. Using this combination of experiments and numerical simulations on both the macro- and the micro-scale, it is possible to predict the evolution of damage strain rates for different loading conditions. Therefore, the procedure can be seen as an efficient tool to obtain data for validation and quantification of stress state dependence of damage and failure criteria and associated evolution laws in phenomenological continuum models.

REFERENCES

[1] Borvik, T., Hopperstad, O.S., Berstad, T. On the influence of stress triaxiality and strain rate on the behavior of a structural steel. Part II. Numerical study, *Eur. J. Mech. A/Solids*(2003) **22**: 15-32.

[2] Bao, Y., Wierzbicki, T. On fracture locus in the equivalent strain and stress triaxialityspace, *Int. J. Mech. Sci.*(2004) **46**: 81-98.

[3] Bonora, N., Gentile, D., Pirondi, A., Newaz, G. Ductile damage evolution under triaxial state of stress: theory and experiment, *Int. J. Plast.*(2005) **21**: 981-1007.

[4] Oh, C.K., Kim, Y.J., Park, J.M., Baek, J.H., Kim, W.S. Development of stress-modified fracture strain for ductile failure of API X65 steel. *Int. J. Fract.*(2007) **143**: 119-133.

[5] Bai, Y., Wierzbicki, T. A new model of metal plasticity and fracture with pressure and Lode dependence, *Int. J. Plast.*(2008) **24**: 1071-1096.
[6] Brünig, M., Chyra, O., Albrecht, D., Driemeier, L., Alves, M. A ductile damage criterion at various stress triaxialities, *Int. J. Plast.*(2008) **24**: 1731-1755.
[7] Gao, X., Zhang, T., Hayden, M., Roe, C. Effects of the stress state on plasticity and ductile failure of an aluminum 5083 alloy. *Int. J. Plast.*(2009) **25**: 2366-2382.
[8] Brünig, M., Albrecht, D., Gerke, S. Numerical analyses of stress-triaxiality-dependent inelastic deformation behaviour of aluminium alloys, *Int. J. Damage Mech*. (2011) **20**: 299-317.
[9] Needleman, A. Void growth in an elastic-plastic medium. *J. Appl. Mech.*(1972) **39**: 964-970.
[10] Becker, R., Smelser, R.E., Richmond, O. The effect of void shape on the development of damage and fracture in plane-strain tension. *J. Mech. Phys. Solids*(1989) **37**: 111-129.
[11] Brocks, W., Sun, D.-Z., Hönig, A. Verification of the transferability of micromechanical parameters by cell model calculations with visco-plastic material. *Int. J. Plast.* (1995) **11**: 971-989.
[12] Kuna, M., Sun, D.Z. Three-dimensional cell model analyses of void growth in ductile metals. *Int. J. Fract*. (1996) **81**: 235-258.
[13] Zhang, K.S., Bai, J.B., Francois, D. Numerical analysis of the influence of the Lode parameter on void growth. *Int. J. Solids Struct*. (2001) **38**: 5847-5856.
[14] Kim, J., Gao, X., Srivtsan, T.S. Modeling of crack growth in ductile solids: a three-dimensional analysis. *Int. J. Solids Struct*. (2003) **40**: 7357-7374.
[15] Gao, X., Wang, T., Kim, J. On ductile fracture initiation toughness: Effects of void volume fraction, void shape and void distribution. *Int. J. Solids Struct*. (2005) **42**: 5097-5117.
[16] Gao, X., Zhang, G., Roe, C. A study on the effect of the stress state on ductile fracture. *Int. J. Damage Mech*. (2010) **19**: 75-94.
[17] Brünig, M., Gerke S., Hagenbrock, V. Micro-mechanical numerical studies on the stress state dependence of ductile damage, In: H. Altenbach, S. Kruch (eds.), *Advanced Materials Modelling for Structures*, Springer-Verlag Berlin Heidelberg (2013) 87-96.
[18] Brünig, M., Gerke S., Hagenbrock, V. Micro-mechanical studies on the effect of the stress triaxiality and the Lode parameter on ductile damage. *Int. J. Plast.* (2013) doi:10.1016/j.ijplas.2013.03.012.
[19] Brünig, M. An anisotropic ductile damage model based on irreversible thermodynamics, *Int. J. Plast*. (2003) **19**: 1679-1713.
[20] Bao, Y., Wierzbicki, T. On the cut-off value of negative triaxiality for fracture, *Eng. Frac. Mech*. (2005) **72**: 1049-1069.
[21] Khan, A.S., Liu, H. A new approach for ductile fracture prediction on Al 2024-T351 alloy. *Int. J. Plast.* (2012) **35**: 1-12.
[22] Khan, A., Liu, H. A new approach for ductile fracture prediction on Al 2024-T351 alloy. *Int. J. Plast.* (2012) **35**: 1-12.